Pressure studies and magnetic properties of poly-phase Fe-Te-Se systems

Steffen Hartwig[a,*], Sven Landsgesell[a], André Sokolowski[a], Norbert Schäfer[a], Daniel Abou-Ras[a], Bernd Büchner[b,c], Michael Schulze[b], Christian G. F. Blum[b], Sabine Wurmehl[b,c], Karel Prokeš[a]

[a]*Helmholtz-Zentrum Berlin für Materialien und Energie, Hahn-Meitner Platz 1, 14109 Berlin, Germany*
[b]*Leibniz-Institut für Festkörper- und Werkstoffforschung (IFW) Dresden, D-01069 Dresden, Germany*
[c]*Institut für Festkörperphysik, Technische Universität Dresden, Dresden, Germany*

Abstract

To study the influence of the sample preparation procedure on the superconducting properties of $FeSe_xTe_{1-x}$, we have grown two $FeSe_{0.4}Te_{0.6}$ crystals and investigated their superconducting properties. One of the crystals possessed a secondary phase of $Fe_3Se_{2.1}Te_{1.8}$, while the other was a high-quality $FeSe_{0.4}Te_{0.6}$ single crystal. We have checked the sample compositions and phases via energy dispersive x-ray spectroscopy to obtain a more sophisticated picture of the inclusions. Our susceptibility measurements under hydrostatic pressure show that neither pressure up to 9 kbar nor stress is sufficient to obtain a superconducting state in the homogeneous crystal. The critical temperature of two-phase $FeSe_{0.4}Te_{0.6}$ increases at 8.9 kbar from 12.3 K to T_c=17.9 K. Therefore, we conclude that inhomogeneities are a necessary feature for providing superconductivity in this iron chalcogenide system. We have prepared $Fe_3Se_{2.1}Te_{1.8}$ polycrystals and studied their magnetic properties for comparison.

Keywords: Superconductivity, Iron chalcogenide, Pressure studies

1. Introduction

Because of the magnetic properties of iron, for a long time superconductivity in iron-based compounds was assumed to be impossible. But since the surprising discovery of superconductivity in $La(O_{1-x}F_x)FeAs$ (1111) a large variety of superconducting materials have been found [1]. Besides (122) compounds like $SrFe_2As_2$ or (111) compounds like LiFeAs, the investigation of $FeSe_xTe_{1-x}$ plays a special role since this basic (11) iron pnictide is considered as the simplest member of this class of materials. [2][3]

---

*Corresponding author
Email address: steffen.hartwig@helmholtz-berlin.de (Steffen Hartwig)

$FeSe_xTe_{1-x}$ adopts a crystal structure with space group $P4/nmm$ (No. 129) and cell parameters $a \approx 3.8\AA$ and $c \approx 6.1\AA$. [4][5] Except for stoichiometric FeTe, traces of filamentary superconductivity can be found for all x-values[5] (even for x=1 with T_c=8 K). Bulk superconductivity can only be obtained for $x \geq 0.29$.[6] The highest transition can be reached for $x \approx 0.4$ with $T_c \approx 14$ K. In any case, T_c is strongly dependent on pressure.[7][8][9]

Many reports have shown the superconducting features and declared a very sensitive behaviour to iron deficiencies.[5][10] Most of them observed traces of a secondary, iron-containing phase.[11][12][13] So far, most works assumed negligible contributions of those minor secondary phase(s) to the observed physical properties of the Fe-Se-Te bulk samples.

However, several recent publications revealed that the impact of those secondary phases must be taken into account to interpret and understand the properties of the Fe-Se-Te system. In particular, it turns out that those foreign phases are a mandatory ingredient for the observation of bulk superconductivity. [14][15] Neither the sometimes observed $Fe_3Se_{2.1}Te_{1.8}$-inclusions[4] nor the in some publications mentioned Fe_7Se_8, which are crystallographically similar and differ only in ordered vacancies, are superconducting themselves. Therefore, an explanation of the interplay between these compounds can reveal a new approach to explain superconductivity in iron chalcogenides.[13]

We have grown two different types of $FeSe_{0.4}Te_{0.6}$ crystals by applying different cooling procedures to study the relation between the secondary phases and superconductivity in this system. One sample shows bulk superconducting properties (SC) but contains inclusions of a secondary phase, while the second sample is homogenous and not superconducting (NSC). We analyzed the differences of both samples using x-ray diffraction and susceptibility measurements under pressure and strain. Additionally a sample of the observed inclusions was grown and investigated as well.

2. Sample Preparation

Two types of single crystals have been grown using metallic iron (Fe pieces, 99.7%), tellurium (Te pieces, 99.999%) and selenium (Se shots, 99.999%) in a stoichiometric melt by applying a modified Bridgman-method. At the beginning of the preparation, both temperature zones were heated with the same rate of 5 K/min to 650 °C and held for twelve hours to allow for pre-reacting of the elements, followed by heating with 5 K/min to 860 °C. A dwell time of 24 h was used to ensure a homogeneous melt. Afterwards, the samples were cooled to room temperatures at different rates. The fast-cooled with 2 K/min and the slow-cooled with 0.2 K/min. These velocities are essential for the (electrical) properties.[16] For a more detailed description of the sample preparation we refer to a previous publication. [4]

The composition and purity has been checked via X-ray powder diffraction using a Bruker D8 (Cu-Kα) diffractometer and EDX measurements.

For the synthesis $Fe_3Se_{2.1}Te_{1.8}$ sample, the constituent pure elements were sealed in appropriate stoichiometry in a quartz ampule and heated to 800 °C.

The melt stayed at this temperature for 7 days, before it was cooled down to room temperature within one hour. The resulting sample was polycrystalline and was pulverized for further studies.

3. Techniques

Analyses by scanning electron microscopy were performed on freshly cleaved and polished single crystals, since the material surface quality deteriorates significantly with time exposed to air. Two microscopes were used: a Philips XL30 equipped with an microprobe analyzer (energy-dispersive X-ray spectrometry, EDX) for semiquantitative elemental analysis, and a Zeiss UltraPlus with a combined electron backscatter diffraction (EBSD) and EDX measurement system (Oxford Instruments AZtec, using NordlysNano EBSD and 80 mm^2 XMax X-ray detectors). The acceleration voltage applied was 15 kV.

X-ray powder patterns have been obtained by use of a Bruker D8 (Cu Kα) powder diffractometer on a rotating powder sample at room temperature and have been analyzed with the Jana2006-program.[17] In the case of $FeSe_xTe_{1-x}$, which forms plate-like single crystals with c-axis direction orthogonal to the surface, the powder data had to be corrected for a preferred orientation. This is a procedure not necessary for the Fe_3Se_4-type of material.

Magnetic property measurements have been performed on a Quantum Designs 7T MPMS DC vibrating sample magnetometer (VSM) with oven option in the temperature range 2-600 K in a magnetic field up to 7 T under zero-field (zf) and non zero-field (nzf) conditions. For high temperature measurements the powder sample was glued within ZIRCAR-cement. Contribution of two data sets causes a minor gap in the magnetization data. At temperatures above 500 K selenium reacts with the copper foil, which is used as heat-shield, but due to the cement this affects only a minor part of the sample.

Additionally, AC susceptibility has been measured using a self-made pick-up coil system. This first order gradiometer is specialized for the usage of large and heavy pressure cells. The low temperature measurements have been performed in a standard orange cryostat down to 1.6 K.

For pressure measurements a copper-beryllium clamped-type pressure cell was used. The sample was embedded in spindle oil as a pressure-transmitting-medium. Via resistivity measurements of a Manganin sensor pressure has been determined at room temperature. The pressure difference to the lowest temperature is well known and amounts to 2 kbar. Additionally, some measurements with applied stress by bending the samples were performed.

Although the influence of the various parts of the pressure cell for the AC susceptibility measurements is not negligible, the detection of bulk superconductivity is a straightforward job. Filamentary superconductivity in the pure $FeSe_{0.4}Te_{0.6}$ has been detected earlier by resistivity measurements, however, its volume is too small to be visible in our AC susceptibility experiments.[4]
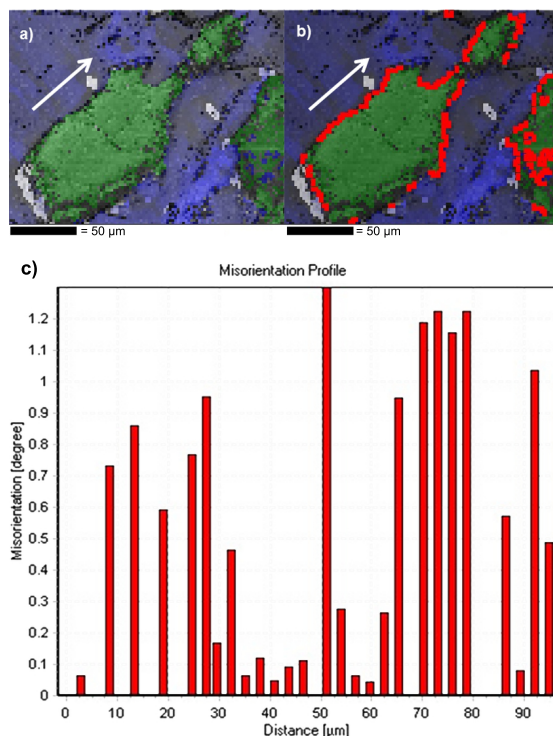
Figure 1: a) EBSD Euler angle Φ_2 distribution coloring in blue indicating the orientation of the unit cells. Secondary phase colored in green. b) Additional phase boundaries colored in red. c) Misorientation profile along line indicated by the arrow showing slight deviations in Φ_2 which indicates strain within phase.
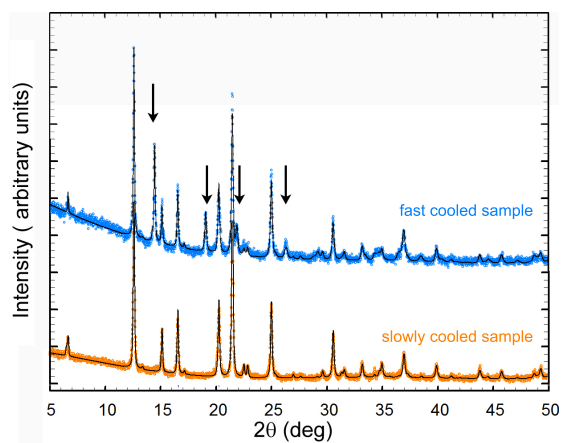

Figure 2: X-ray diffractogram of both samples. The homogeneous slowly cooled sample at the bottom has orange dots. Blue dots at the top mark the inhomogeneous fast-cooled sample. The black lines represent Rietveld refinements [4]. Additional peaks due to impurities of $Fe_3Se_{2.1}Te_{1.8}$ in the fast-cooled sample are clearly visible and indicated by arrows.
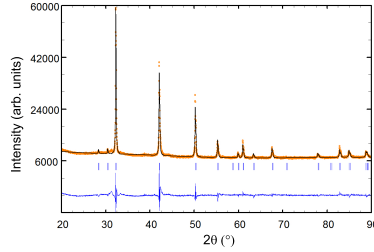
Figure 3: X-ray diffraction pattern of a $Fe_3Se_{2.1}Te_{1.8}$ powder sample. The blue line marks the difference between fit and data (see also Table 1). This material clearly explains the difference of the the fast and slowly cooled samples x-ray measurements shown previously in Fig.2.
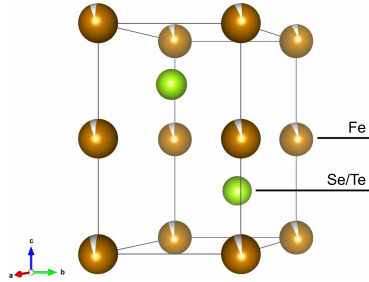

Figure 4: One unit cell of the hexagonal crystal structure of $Fe_3Se_{4-x}Te_x$. Iron is represented by the brown spheres, selenium and tellurium by green ones.

$Fe_3Se_{2.1}Te_{1.8}$				
Space group:	P 6_3/m m c			
R_{Main}	6.51			
Cell parameter:		Occupancy:		
$a(\mathring{A})$	3.7127(2)	Fe	0.7692(0)	
$b(\mathring{A})$	3.7127(2)	Se	0.5385(0)	
$c(\mathring{A})$	5.6708(4)	Te	0.4615(0)	
Atomic positions:				
Label:	site:	x	y	z
Fe	2a	0	0	0
Se	2c	$\frac{1}{3}$	$\frac{2}{3}$	$\frac{1}{4}$
Te	2c	$\frac{1}{3}$	$\frac{2}{3}$	$\frac{1}{4}$

Table 1: Crystal structure parameters of the $Fe_3Se_{2.1}Te_{1.8}$ powder at room temperature obtained by x-ray diffraction.

4. Results

EBSD reveals for the fast cooled sample a two-phase structure of $Fe_3Se_{2.1}Te_{1.8}$ inclusions in a $Fe_{1.036}Se_{0.377}Te_{0.623}$ matrix. On the other hand, the slowly cooled sample is a high quality single crystal of $Fe_{0.96}Se_{0.4}Te_{0.6}$ without this secondary phase. Obviously, there is a slight deficiency of iron at the surface of the slowly cooled sample, which we explain with the polishing process. Previous neutron diffraction experiments with the same crystal do not show this deficit in the bulk.[4] In Fig.1 an excerpt of an EBSD map is shown, which gives a closer look to the inclusions with the surrounding matrix. In previous measurements, inhomogeneities in chemical composition and stoichiometry are clearly visible as manifested in the chemical contrast between matrix and secondary phase.[4] In addition, areas within the matrix which are in the proximity of the secondary phase exhibit a distribution of crystal direction demonstrated by the varying blue tones in the EBSD map. Apparently, the secondary phase reduces the regularity of the matrix crystal and alters the cell parameters and crystallographic orientation. With this, the matrix suffers from stress and strain induced by the secondary phase. Please note that there is no distinct relationship between the orientation of the matrix and the secondary phase.

While XRD patterns of the slowly cooled sample show a perfect single-crystalline $Fe_{1.035}Se_{0.344}Te_{0.655}$ phase, the fast-cooled sample exhibits significant inhomogeneities (Fig. 2) due to a second phase. The secondary phase was found to be $Fe_3Se_{2.1}Te_{1.8}$.[4] Both the slowly cooled sample and the matrix of the fast-cooled sample order in the P4/nmm space group (No.129).

The crytal structure of the inclusions is, however, more difficult to refine. To obtain more information this second phase has been prepared separately and analyzed as well. The XRD pattern of this material is shown in Fig.3 and the results of the corresponding Rietveld refinement are given in Table 1. Several deviations in stoichiometry may occur in the polycrystalline melt, so the peak shape is not optimally defined. However, the similarity to the secondary phase shown in Fig.2 is obvious. $Fe_3Se_{2.1}Te_{1.8}$ orders in an NiAs type crystal structure with the space group P6$_3$/mmc (Fig. 4). A less symmetric monoclinic space group I2/m like in Fe_7Se_8 has been considered during the refinement as well. However, the monoclinic angle β differed only slightly from 90°, indicating a higher symmetry. Therefore, we used the hexagonal compound Fe_3Se_4, where selenium and tellurium share the same crystallographic position, as a basis for the refinement. Please note that the lattice constants are somewhat larger than for the pure Fe_3Se_4 due to the substitution of Se by Te, as expected.

Previous physical property measurements revealed that this inhomogeneous fast-cooled sample shows bulk-superconductivity (Fig. 5).[4][14] On the other hand, Fig.5 surprisingly shows the occurrence of only spurious superconductivity in the slowly cooled sample. Here the fc and zfc curves just split up slightly at T_c. Both curves increase while cooling until 3.5 K, where the zf-curve reaches a maximum and drops.[4]

In order to shed light on the properties of the secondary phase and its relation to and impact on the superconductivity, we prepared a sample with
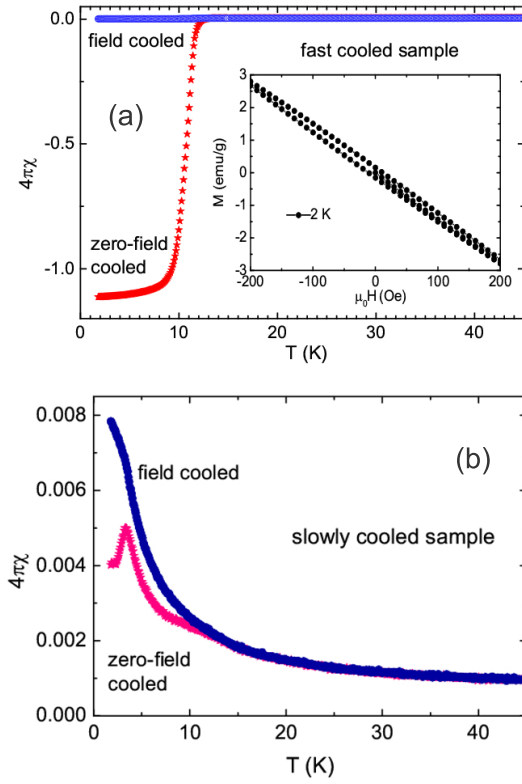
Figure 5: (a) The temperature dependence of the volume magnetic susceptibility of the inhomogeneous SC sample measured under field cooled (fc) and zero field cooled (zfc) conditions with the magnetic field (20 Oe) aligned along the a-b plane. The pure diamagnetic signal measured at 2 K as function of Field is shown in the inset. (b) The magnetic field dependence of the magnetization curves at 2 K measured on zero-field cooled SC and NSC samples.[4]
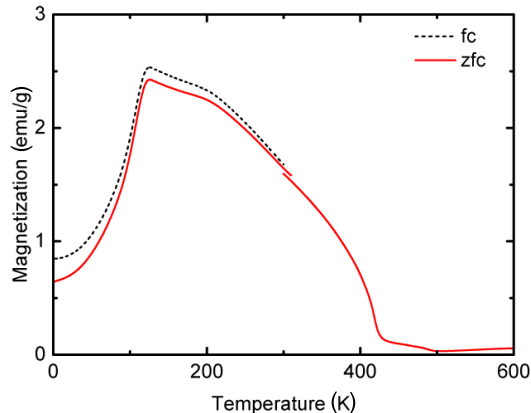
Figure 6: The temperature dependence of the magnetization of $Fe_3Se_{2.1}Te_{1.8}$ with an applied field of 1000Oe. The black line represents a field cooled, the red line represents a zero field cooled measurement. For the high-temperature measurements the sample had to be glued on ZIRCAR-cement instead of GE-Varnish. Therefore a slight gap in the magnetization data is visible around room temperature.

$Fe_3Se_{2.1}Te_{1.8}$ composition which matches the secondary phase. Susceptibility measurements of the material show an antiferromagnetic behaviour with T_N=109 K followed by a notch in magnetization data at 200 K and final transition to paramagnetism at 425 K (Fig. 6). Both, Fe_3Se_4 and Fe_7Se_8, are well studied and documented. These iron selenides show, according to literature, a very composition sensitive behaviour with a para-ferrimagnetic transition between 225 K and 460 K as well as a ferri-antiferromagnetic transition between 130 K and 210 K. [18][19] Although there is yet no investigation of neither the similar compounds Fe_3Te_4 and Fe_7Te_8 nor the properties of a Se-Te mixture, our results show a high similarity to the mentioned iron selenides, since the multiple phase transitions are visible at comparable temperatures. Apparently, there is no sign of bulk superconductivity. Therefore, the assumption that these inclusions themself are the cause of superconductivity in the fast-cooled sample can be excluded. Some groups mentioned a phase transition of their superconducting $FeSe_xTe_{1-x}$ at approximately 130 K and referred this to various distortions.[11][13] Most likely, the inclusions we present are the origin of the reported transitions and, since these distortions are mentioned frequently, an intrinsic feature necessary for bulk superconductivity.

In the following, we will discuss evolution of superconductivity in the homogenous, slowly cooled sample and inhomogeneous fast-cooled sample as function of pressure monitored by ac susceptibility measurements. The induced AC voltage (real part) of the pick-up coil system for the fast-cooled sample as a function of temperature is shown in Fig.7. These data were measured on heating. Maximal voltage of the curve is varying with different pressures, since changing the pressure alters the geometry within the coil system. Sharp increases of the voltage mark the superconducting transition. This transition gets broader
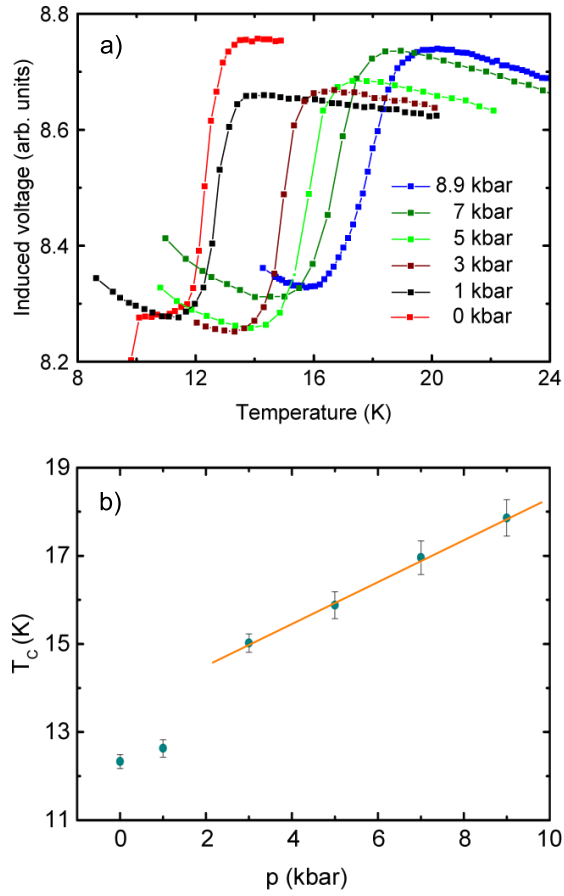
Figure 7: a) Measurement of the induced voltage at the superconducting transitions via AC susceptibility. The zero-pressure data (red) deviates from the other curves, because the non-closed pressure cell in this case leads to a different magnetical background and therefore to a different voltage range. Therefore the voltage is given in arbitrary units. b) Pressure dependence of the critical superconducting temperature T_c of the inhomogeneous fast-cooled $FeSe_{0.4}Te_{0.6}$-sample.

at higher pressure, which is expected considering the samples inhomogeneities. The fast-cooled sample exhibit at ambient pressure a superconducting transition at T_c=12.3 K. With increasing pressure, the critical temperature grows, after initially strong pressure dependence, linearly with 0.47 K/kbar and shifts to T_c=17.9 K at 9 kbar (Fig. 7). This behaviour stands in good agreement with the literature.[9] The monotonic increase of T_c indicates that the pressure is still far from a reported transition to a different monoclinic structure, which leads to a reduced critical temperature. [5][8][9] The shape of the transition temperature development for $FeSe_xTe_{1-x}$ crystals is well documented, although the absolute values are very sensitive to the exact composition.

It has been reported for $FeSe_xTe_{1-x}$ even with suboptimal stoichiometry and therefore usually non-superconducting properties that a transition can be induced by pressure[8]. Surprisingly, the slowly cooled sample did not became superconducting even with pressure up to 9 kbar. Additional stress due to bending of the sample yield the same reults. In literature the maximal critical temperature is mentioned to be close to 30 kbar, which is considerably higher than the highest pressure we have applied. However, this maximum is rather broad and the strongest pressure dependence up to 1 K/kbar has been detected below 10 kbar.[5][9][7] It means that the slight off-stoichiometry of our slowly cooled sample is not the cause of the absence of superconductivity even under pressure.

5. Summary

We have shown that there is no trace of bulk superconductivity in perfect $FeSe_{0.4}Te_{0.6}$ single crystals even with applied pressure and stress. On the contrary, two-phased $FeSe_{0.4}Te_{0.6}$ exhibits superconducting properties that are in agreement with literature.[6] We have found that the secondary phase itself does not exhibit any superconducting phase transition. Therefore, we claim that the connection of these two materials may be a necessary ingredient for superconductivity. Many publications claim the sensitivity of the material to iron amount.[4][10] The formation of the secondary phase during the growing process, which contains less iron per unit cell than the stoichiometric compound $FeSe_{0.4}Te_{0.6}$, could lead to significant local distortions of single crystalline matrix. Additionally, the mismatch between matrix and inclusions cannot be ignored completely, although stress did not affect our slowly cooled sample's electrical properties. For example, the induced strain in the material certainly leads to a variation of the distance of the pnictogen ion to the iron-layers in the $FeSe_{0.4}Te_{0.6}$ crystal structure. This distance has been regarded as a control parameter for superconductivity in iron-based systems.[9][20] In conclusion, we argue that local distortions of the crystal structure (including the stoichiometry) caused by the secondary phase are the driving element of the SC-phase transition.

6. Acknowledgment

[1] Y. Kamihara, T. Watanabe, M. Hirano, H. Hosono, Journal of the American Chemical Society 130 (11) (2008) 3296–3297. `doi:10.1021/ja800073m`.

[2] P. L. Alireza, Y. T. C. Ko, J. Gillett, C. M. Petrone, J. M. Cole, G. G. Lonzarich, S. E. Sebastian, Journal of Physics: Condensed Matter 21 (1) (2009) 012208.

[3] X. Wang, Q. Liu, Y. Lv, W. Gao, L. Yang, R. Yu, F. Li, C. Jin, Solid State Communications 148 (1112) (2008) 538 – 540. `doi:http://dx.doi.org/10.1016/j.ssc.2008.09.057`.

[4] M. Schulze, K. Prokes, S. Hartwig, N. Schfer, S. Landsgesell, C. Blum, D. Abou-Ras, M. Hacisalihoglu, E. Ressouche, B. Ouladdiaf, A. Bachmann, C. Hess, B. Buechner, S. Wurmehl, To be published.

[5] B. Sales, A. Sefat, M. McGuire, R. Jin, D. Mandraus, Y. Mozharivskyj, Phys. Rev. B 79 (2009) 094521. `doi:10.1103/PhysRevB.79.094521`.

[6] T. J. Liu, J. Hu, B. Qian, D. Fobes, Z. Q. Mao, W. Bao, M. Reehuis, S. A. J. Kimber, K. Proke, S. Matas, D. N. Argyriou, A. Hiess, A. Rotaru, H. Pham, L. Spinu, Y. Qiu, V. Thampy, A. T. Savici, J. A. Rodriguez, C. Broholm, Nature Materials 9 (1965) 716. `doi:http://dx.doi.org/10.1038/nmat2800`.

[7] H. Takahashi, H. Takahashi, T. Tomita, H. Okada, Y. Mizuguchi, Y. Takano, S. Matsuishi, M. Hirano, H. Hosono, Japanese Journal of Applied Physics 50 (5S2).

[8] Y. Mizuguchi, F. Tomioka, S. Tsuda, T. Yamaguchi, Y. Takano, Applied Physics Letters 93 (2008) 152505.

[9] N. Gresty, Y. Takabayashi, A. Ganin, M. MacDonald, et al., J. Am. Chem. Soc.s 46 (2009) 16944. `doi:10.1021/ja907345x`.

[10] M. Bendele, P. Babkevich, S. Katrych, S. N. Gvasaliya, E. Pomjakushina, K. Conder, B. Roessli, A. T. Boothroyd, R. Khasanov, H. Keller, Phys. Rev. B 82 (2010) 212504. `doi:10.1103/PhysRevB.82.212504`.

[11] A. V. Fedorchenko, G. E. Grechnev, V. A. Desnenko, A. S. Panfilov, S. L. Gnatchenko, V. V. Tsurkan, J. Deisenhofer, H.-A. Krug von Nidda, A. Loidl, D. A. Chareev, O. S. Volkova, A. N. Vasiliev, Low Temperature Physics 37 (1) (2011) 83–89. `doi:http://dx.doi.org/10.1063/1.3552132`.

[12] B. Joseph, A. Iadecola, A. Puri, L. Simonelli, Y. Mizuguchi, Y. Takano, N. L. Saini, Phys. Rev. B 82 (2010) 020502. `doi:10.1103/PhysRevB.82.020502`.

[13] M. Bendele, S. Weyeneth, R. Puzniak, A. Maisuradze, E. Pomjakushina, K. Conder, V. Pomjakushin, H. Luetkens, S. Katrych, A. Wisniewski, R. Khasanov, H. Keller, Phys. Rev. B 81 (2010) 224520. `doi:10.1103/PhysRevB.81.224520`.

[14] A. Wittlin, P. Aleshkevych, H. Przybylinska, D. Gawryluk, P. Dluzewski, M. Berkowski, R. Puzniak, M. Gutowska, A. Wisniewski, Superconductor Science and Technology 25 (2012) 065019. `doi:doi:10.1088/0953-2048/25/6/065019`.

[15] L. Vinnikov, A. Radaev, I. Veshchunov, A. Troshina, Y. Liu, C. Lin, A. Boris, JETP Letters 93.

[16] D. Louca, J. Yan, A. Llobet, R. Arita, Physical Review B 84 (2011) 054522. `doi:10.1103/PhysRevB.84.054522`.

[17] V. Petříček, M. Dušek, L. Palatinus, Crystallographic computing system jana2006: General features, Z. Kristallogr. 229 (2014) 345–352. `doi:10.1515/zkri-2014-1737`.

[18] K. Hirakawa, Journal of the Physical Society of Japan 12 (8) (1957) 929–938. `doi:10.1143/JPSJ.12.929`.

[19] P. Terzieff, K. Komarek, Monatshefte für Chemie / Chemical Monthly 109 (5) (1978) 1037–1047. `doi:10.1007/BF00913006`.

[20] K. Kuroki, H. Usui, S. Onari, R. Arita, H. Aoki, Phys. Rev. B 79 (2009) 224511. `doi:10.1103/PhysRevB.79.224511`.